Marine Geophysical Researches (2004) 25:305–319
DOI 10.1007/s11001-005-1338-8

The Agulhas Ridge, South Atlantic: the peculiar structure of a fracture zone

Gabriele Uenzelmann-Neben* & Karsten Gohl
*Alfred Wegener Institute for Polar and Marine Research, Postfach 120161, D-27515 Bremerhaven, Germany; *Corresponding author (Phone: +49-471-4831-1208; Fax: +49-471-4831-1271; E-mail: uenzel@awi-bremerhaven.de)*

Received 30 October 2003; accepted 30 October 2004.

Key words: Agulhas-Falkland Fracture Zone, transverse ridge, Agulhas Ridge, South Atlantic, seismic reflection and refraction data, Discovery Hotspot, Shona Hotspot, Bouvet Hotspot, ODP Leg 177

Abstract

The Agulhas Ridge is a prominent topographic feature that parallels the Agulhas-Falkland Fracture Zone (AFFZ). Seismic reflection and wide angle/refraction data have led to the classification of this feature as a transverse ridge. Changes in spreading rate and direction associated with ridge jumps, combined with asymmetric spreading within the Agulhas Basin, modified the stress field across the fracture zone. Moreover, passing the Agulhas Ridge's location between 80 and 69 Ma, the Bouvet and Shona Hotspots may have supplied excess material to this part of the AFFZ thus altering the ridge's structure. The low crustal velocities and overthickened crust of the northern Agulhas Ridge segment indicate a possible continental affinity that suggests it may be formed by a small continental sliver, which was severed off the Maurice Ewing Bank during the opening of the South Atlantic. In early Oligocene times the Agulhas Ridge was tectono-magmatically reactivated, as documented by the presence of basement highs disturbing and disrupting the sedimentary column in the Cape Basin. We consider the Discovery Hotspot, which distributes plume material southwards across the AAFZ, as a source for the magmatic material.

Introduction

Oceanic fracture zones are long, linear bathymetric structures in ocean basins, which normally follow arcs of small circles on the Earth's surface from the sea-floor spreading ridge toward the continental margins (Bonatti and Crane, 1984). They form in prolongation of transform faults and are aseismic as opposed to the seismically active transform faults, which lie between spreading ridge segments. Fracture zones can form topographic ridges up to a couple of kilometres high in areas with low sediment cover. The crustal age difference across a fracture zone can be several Ma. Due to their nature as whole crust-penetrating fault systems, fracture zones are suspected of serving as leads for magmatic extrusions. In addition to their tectono-magmatic significance, topographically outstanding fracture zones are of palaeo-oceanographic interest because of their direct effect on the direction and diversion of deep ocean currents.

A fracture zone with one of the largest offsets between crustal segments can be found in the South Atlantic (Figure 1). The Agulhas-Falkland Fracture Zone (AFFZ) spans between the southern margin of South Africa and the northern edge of the Falkland Plateau. Its development began during the early Cretaceous break-up of Gondwana at the separation between Africa and South America (e.g. Ben Avraham et al., 1993, 1997). Before the initial opening of the South Atlantic at about 130 Ma, the Falkland Plateau was located adjacent to South Africa (Labreque and Hayes, 1979; Tucholke et al., 1981). The initial rifting took place north of the AFFZ and east of the Falkland Plateau. By sea-floor spreading anomaly M0 (~109 Ma, Late Albian), an RRR-triple junction had formed by a small ridge jump to the northern end of the present day Agulhas Plateau (Tucholke et al., 1981; Ben Avraham et al., 1997). A second ridge jump at around 83 Ma (isochron 34) placed the spreading axis in the Agulhas Basin farther west. Another

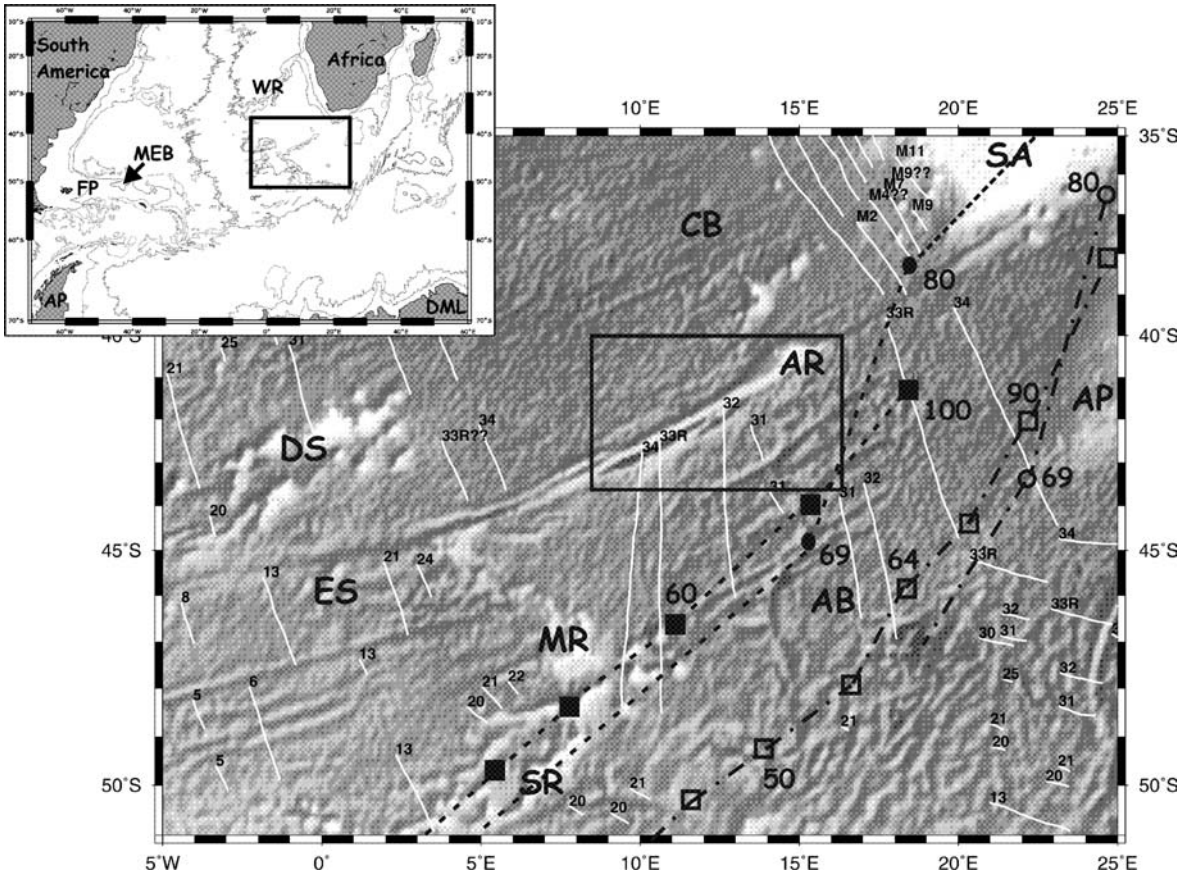

Figure 1. Satellite-derived predicted bathymetric (Smith and Sandwell, 1997) map of the South Atlantic showing magnetic anomalies according to Cande et al. (1989). Tracks of the Bouvet Hotspot (open circles with dot-dashed lines according to Martin, 1987; open squares with dot-dashed lines according to Hartnady and le Roex, 1985) and the Shona Hotspot (filled circles with dashed lines according to Martin, 1987; filled squares with dashed lines according to Hartnady and le Roex, 1985) are included. The numbers indicate the time when the hotspot is assumed to have reached that location. The box refers to the blown-up part shown in Figure 2a, b. AB = Agulhas Basin, AR = Agulhas Ridge, AP = Agulhas Plateau (in insert map Antarctic Peninsula), CB = Cape Basin, DS = Discovery Seamount, DML = Dronning Maud Land, ES = Eastern Seamounts, FP = Falkland Plateau, MEB = Maurice Ewing Bank, MR = Meteor Rise, SR = Shona Ridge, WR = Walvis Ridge.

relocation of the ridge to the Meteor Rise/Islas Orcadas Rise took place around 62 Ma (isochron 27) (Tucholke et al., 1981; Marks and Stock, 2001).

Between 41°–43°S and 16°–9°E, the AFFZ is characterised by a pronounced topographic anomaly, the so-called Agulhas Ridge. It is formed by two parallel ridge segments separated by a central valley (Figure 2a, b). The ridge segments rise more than 2 km above the surrounding seafloor. A similar topographic high can only be found in form of marginal ridges along the continental parts of the AAFZ, namely the Falkland Escarpment at the South American continent (Lorenzo and Wessel, 1997; Bird, 2001) and the Diaz Ridge adjacent to South Africa (Ben Avraham et al., 1993, 1997; Bird, 2001). But the Agulhas Ridge differs from both the Falkland Escarpment and the Diaz Ridge in that (1) it was not formed during the early rift-drift phase, and (2) it separates oceanic crust of different age and not continental from oceanic crust. Thus we expect a different origin.

Up to date, little has been published on the structure of the Agulhas Ridge itself. Research has been concentrated on (1) the plate tectonic reconstruction of the whole South Atlantic (e.g. Barker, 1979; Labreque and Hayes, 1979; Martin and Hartnady, 1986; Stock and Marks,

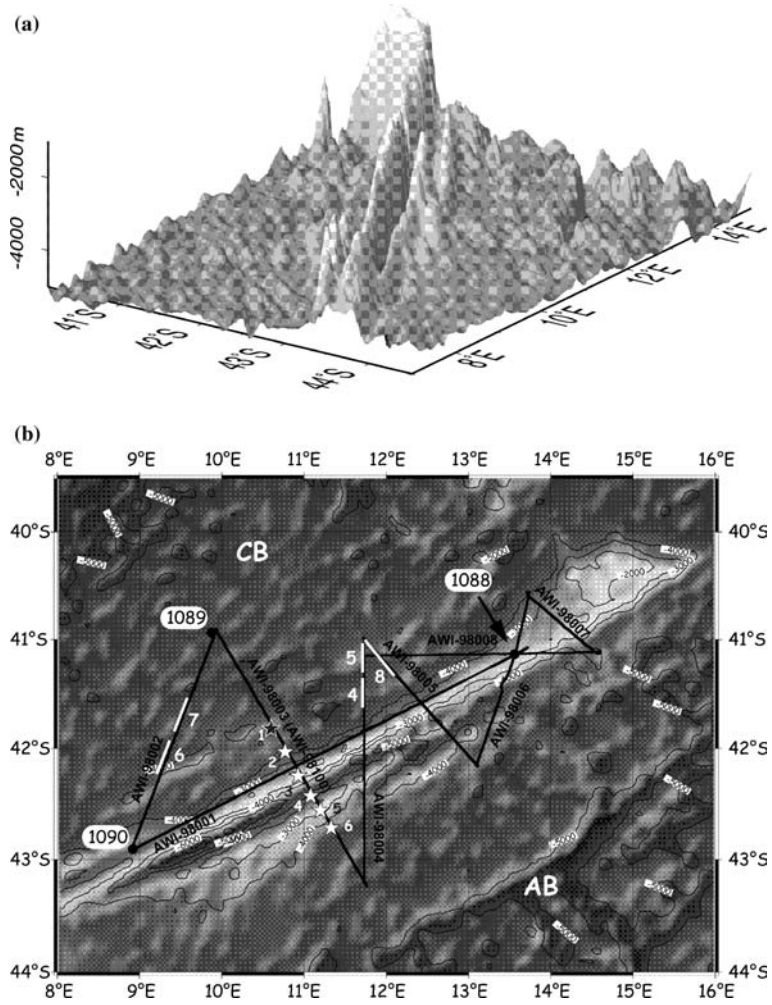

Figure 2. (a) Three dimensional map of the predicted bathymetry derived from satellite altimetry (Smith and Sandwell, 1997), illustrating the asymmetry between the northern and southern parallel ridge segments of the Agulhas Ridge separated by a central valley. (b) Location map of the seismic profiles. The numbered white stars show the locations of the OBH stations used for the refraction/wide-angle data analysis and modelling. One system failed to record (black star). The white bold numbers give the figure numbers of those parts of the seismic lines, which are shown in this paper. The location of ODP Leg 177, Sites 1088, 1089 and 1090, are included (Gersonde et al., 1999).

2001), and (2) the role played by the ridge as an obstacle for oceanic currents (e.g. Gersonde et al., 1999, 2001; Wildeboer Schut et al., 2002). During a seismic campaign in December 1997 and January 1998, carried out by the Alfred Wegener Institute for Polar and Marine Research (AWI) with the chartered RV *Petr Kottsov*, multi-channel seismic reflection profiles with a total length of 2200 km and a deep-crustal refraction/wide-angle reflection profiles were collected (Figure 2b). The profiles cover the Agulhas Ridge and the adjacent parts of the Cape and Agulhas Basins. The reflection lines also connect the three drill sites of Ocean Drilling Project (ODP) Leg 177 on the Agulhas Ridge (Gersonde et al., 1999). Thus, information on the nature and ages of several key reflectors was provided. In this paper, we will present a set of eight high-resolution seismic reflection lines and one seismic refraction/wide-angle reflection profile across the Agulhas Ridge and discuss those data under the scope of deciphering more about the structure and the development of the ridge.

Methods

Seismic reflection data

The high-resolution seismic profile data were collected using two GI-guns™ fired at a nominal interval of 37.5 m, generating reflection signals with recorded frequencies of up to 220 Hz. Each GI-gun™ was fired from a generator chamber of 0.7 l volume to generate the signal, while firing of pressurised air of an injector chamber of 1.7 l volume was delayed to suppress the bubble effect. This provided a vertical resolution of approximately 3.5 m. The data were recorded with a 96-channel 2700 m long streamer with a 2400 m long active section.

Rough weather conditions during data collection called for extensive editing and filtering of noisy traces, especially for large offset dataset. A band-pass filter of 25 Hz to 200 Hz was used for traces with offsets smaller than 700 m. The low-cut frequency has been raised to 55 Hz for larger offsets because low frequency contamination of the data started dominating the signal. A residual source static correction proved to enhance trace-to-trace coherency significantly, which is necessary for a proper velocity analysis. Additional processing steps were carried out to further improve the signal-to-noise ratio of the stacked section by improving the lateral coherence within NMO-corrected CMP records such as a pre-stack f–x deconvolution. This step however has the potential to distort the amplitudes, which is undesirable. Adding 40% of the original data back proved to yield an adequate balance between resolution and preservation of amplitudes.

Seismic refraction/wide-angle data

The data used to derive a structural model of the crust and uppermost mantle across the Agulhas Ridge consist primarily of seismic refraction and wide-angle reflection records from profile AWI-98100 (Figure 2b), along which ocean-bottom hydrophone (OBH) systems were deployed. This profile follows the track of the high-resolution reflection profile AWI-98003. A single 60-l sleeve airgun (Russian-made model PS100) with working pressure of 10 MPa at a water depth of 15 m served as seismic source. The airgun was fired every 60 s, resulting in a shot spacing of approximately 160 m. Airgun signals were recorded by five OBH (type GEOMAR-OBH) systems (stations OBH-2 to OBH-6) with a nominal station spacing of 32 km. The northernmost system at station OBH-1 failed recording. For each OBH, signals were recorded via a single hydrophone onto four channels with different gain factors and at a sample rate of 100 Hz. In addition to the OBH survey, the airguns shots were recorded with the 2400-m streamer as a low-fold multichannel reflection profile. These reflection data underwent standard CMP processing.

Data processing of all OBH records involved band-pass filtering between 4 and 17 Hz. The data quality varies enormously from station to station. While records of OBH-4 show strong P-wave arrivals of up to 70 km offset (Figure 3a), arrivals of OBH-5 can only be observed up to 40 km offset (Figure 3b). However, even in some apparently low quality records, we observe coherent weak-amplitude arrivals from large distances. The difference in quality is only partly due to difficult sea-state conditions. As travel-time modelling later shows, the effect of rough seabed and basement topography along the profile prevents the wave-field to be more evenly distributed.

The travel-time – distance data of relatively large-amplitude OBH arrivals at offsets between 20 and 40 km suggest that reflections from the crust-mantle boundary, or Mohorovičič (Moho) discontinuity (P_mP phases), are recorded at most stations. Intra-crustal reflections are also observed, although their appearance changes from record to record. Some records contain first P-wave arrivals at offsets between 40 and 70 km, which are indicative of upper mantle refractions (P_n).

Structure and distribution of sedimentary column and basement

The Agulhas Ridge forms an elongated structure, which rises more than 3 km above the surrounding seafloor (Figures 2a, b and 4). At its north-eastern end, the ridge is characterised by a 110×185 km^2 wide plateau, whereas in the southwest it consists of two parallel reliefs separated by a broad (about 40 km in width), deep depression (Figures 2 and 4). The facing flanks of the two reliefs are much steeper than the

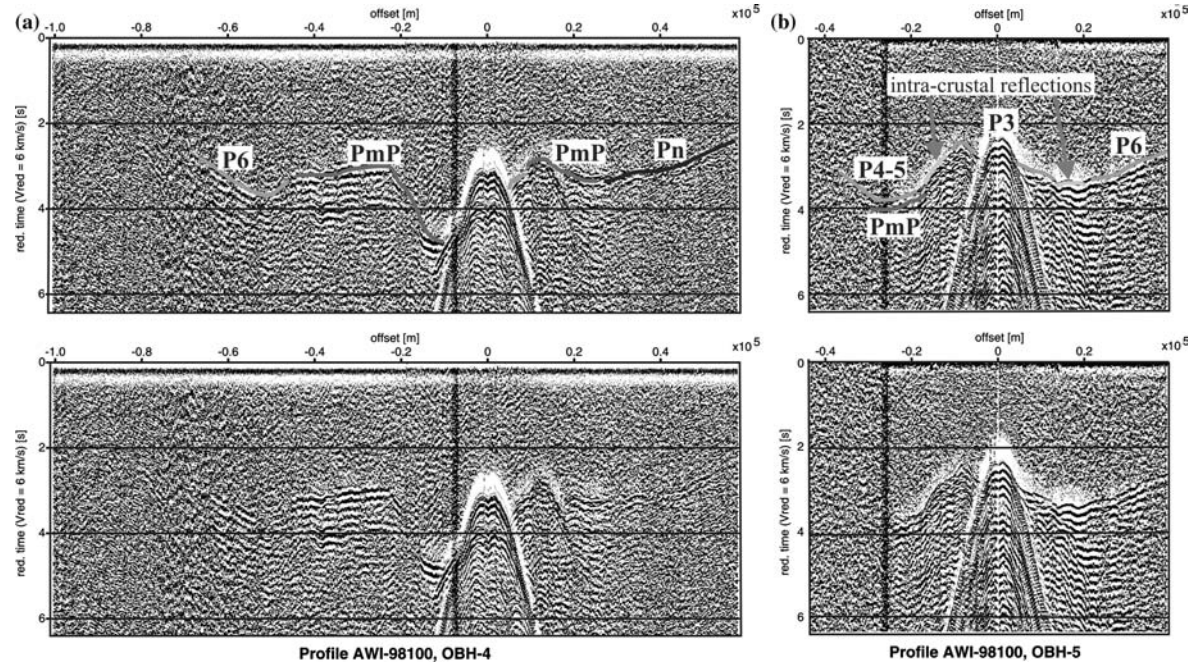

Figure 3. Examples of OBH records along profile AWI-98100 from (a) OBH station 4 and (b) OBH station 5. The upper parts denote annotated travel-time picks, while the lower parts show the complete records. P_{3-6} annotate refracted arrivals from layers with respective model layer numbers. P_mP and P_n mark Moho reflections and uppermost mantle refractions, respectively.

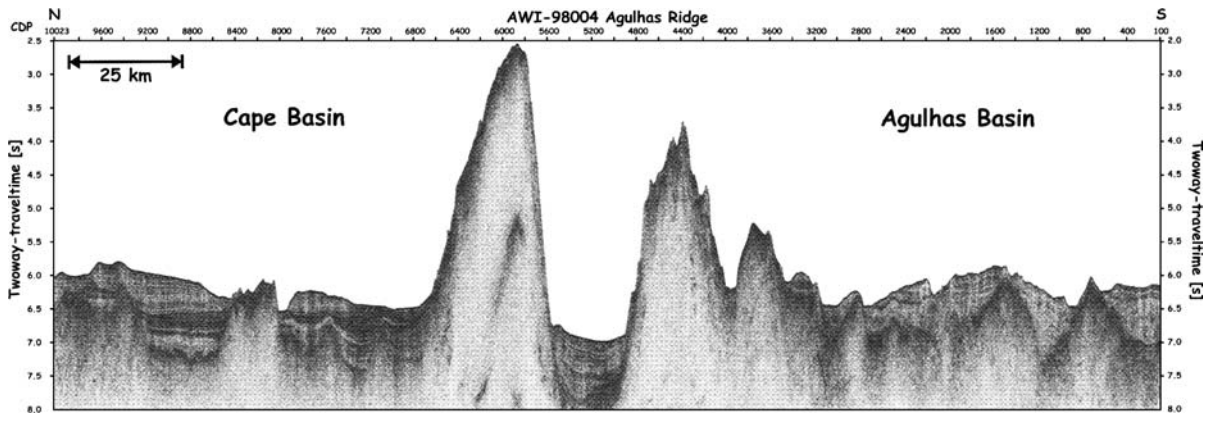

Figure 4. Line AWI-98004 crossing the Agulhas Ridge from north to south. Note the two segments of the ridge separated by the depression. In both Cape and Agulhas Basins basement highs disturbing the sedimentary layers can be observed.

outward lying flanks, thereby indicating the zone where the ridge sheared. The depression is filled with well-layered sediments of at least 1000 ms two-way travel-time (TWT) thickness ($\sim$ 1000 m using $v_P = 2000$ m/s, Figure 4). The ridge itself is of tectono-magmatic origin (Hartnady and le Roex, 1985; Kastens, 1987) and generally shows only a thin sedimentary cover. In a few places, thicker sediment packages can be identified. This is especially true on the northern plateau-like part of the ridge, where we observe a maximum thickness of 1000 ms TWT. Both the Agulhas and Cape Basins show thicker sediment layers in general and contourite sheets consisting of fine-grained bioturbated and homogeneous material (Wildeboer Schut et al., 2002).

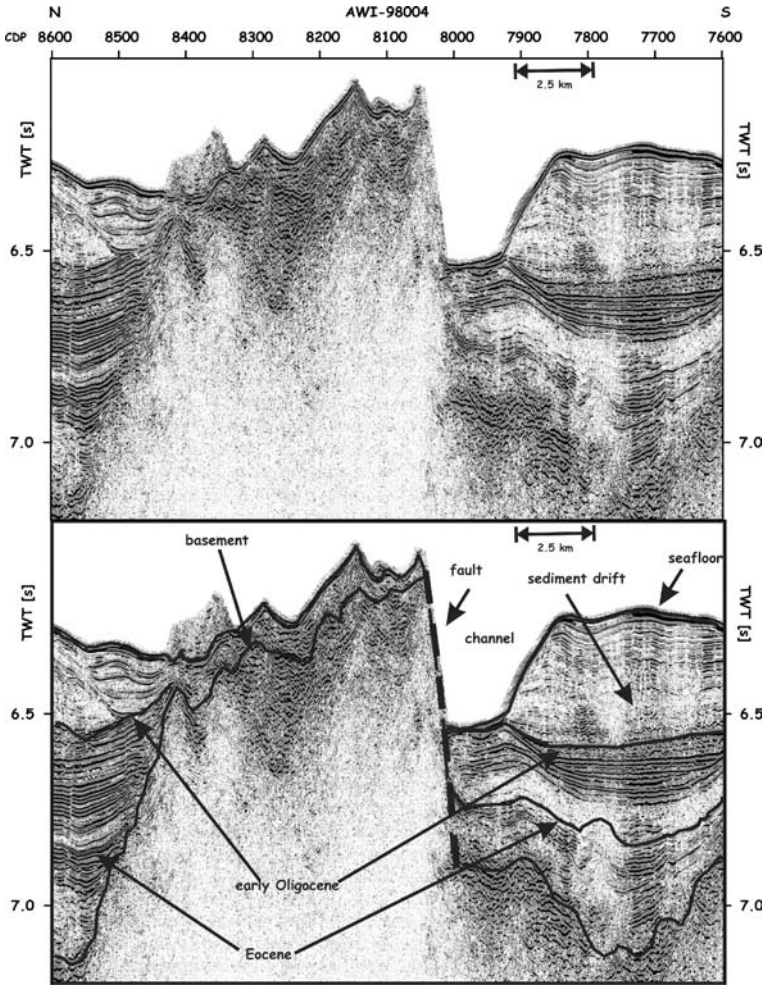

Figure 5. Part of line AWI-98004 showing a raised basement block. South of this block a channel and a drift could develop. For location, see Figure 1. Seismostratigraphy was derived via a correlation with ODP Leg 177 Sites 1088, 1089 and 1090 (Wildeboer Schut et al., 2002).

The seafloor is relatively smooth both north and south of the ridge with a depth about 4500 m. In contrast, the basement shows a number of 'ridges' parallel to the Agulhas Ridge, especially in the Cape Basin. The sedimentary column appears deformed by the basement highs. On line AWI-98004 (Figure 5, CDPs 8000–8500) we observe a basement block, affected by faults dipping towards the south. There, the sedimentary sequence is disrupted and a channel could develop leading to the formation of a sedimentary drift (Wildeboer Schut et al., 2002). The pre-early Oligocene reflectors are pulled-up on both sides of the basement block (mainly on the northern flank), and the basement pierces this sequence between CDPS 8050 and 8400 (Figure 5). This indicates a deformation of the sediments of early Oligocene age.

Another part of line AWI-98004 (Figure 6, CDPs 9000–9700) shows this as well. Here, we see a basement high disrupting the reflectors up to early Oligocene (Figure 6). It is difficult to say whether the younger sequences have been deformed as well. The difference in thickness of the early Oligocene-Miocene unit north and south of the basement high as well as the broadening of the shape of the high within the younger units and the slight relocation towards the North rather point to a post-deformational drape and the influence of currents on the deposition of the

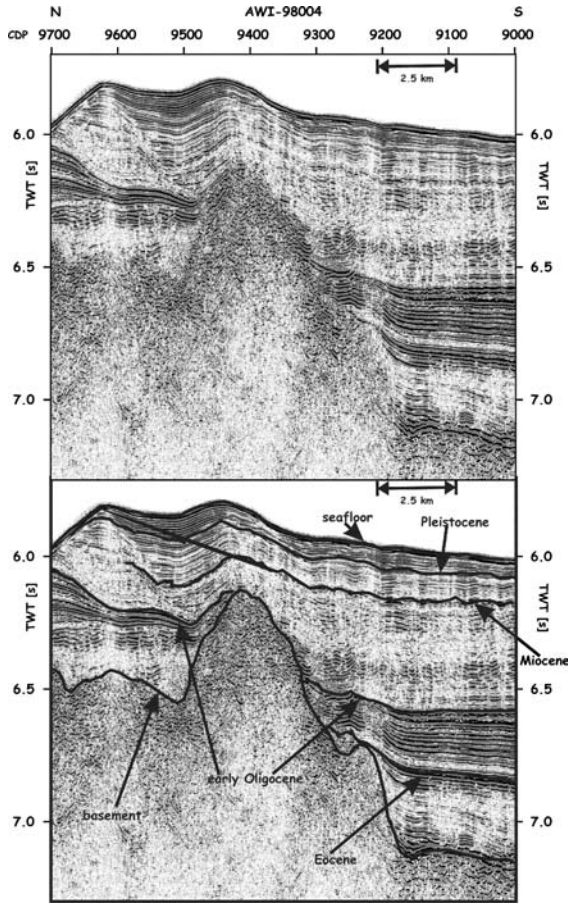

Figure 6. Part of Line AWI-98004 showing a basement high deforming the sedimentary layers. For location, see Figure 1. Seismostratigraphy was derived via a correlation with ODP Leg 177 Sites 1088, 1089 and 1090 (Wildeboer Schut et al., 2002).

post-early Oligocene sedimentary column. Hence, an early Oligocene tectono-magmatic deformation appears plausible. On line AWI-98002 (Figure 7, CDPs 3800–4200) a basement high even pierces the seafloor. The seafloor is thrusted by about 250 ms TWT (~190 m). Again, a small channel could form on the northern side. The sedimentary layers are all disrupted and are much deformed on the southern side of the basement high (Figure 7, CDPs 3800–3900).

Between CDPs 3400 and 3600 on line AWI-98002 (Figure 7), we see another example of a basement high piercing the seafloor. All the seismic lines of our data set show deformed pre-Oligocene deposits draped by a more transparent sedimentary unit.

Observations on line AWI-98002 (Figure 8, CDPs 6250–6500) support this interpretation. There, an intrusion led to a well-defined deformation of the whole sedimentary column. Active erosion at the seafloor in turn removed the younger sedimentary layers and smoothed the seafloor. Immediately south (CDPs 6050–6250), we observe a basement high bounded by two faults with displacements of ~400 ms TWT (300 m) in the south and ~700 ms TWT (525 m) in the north. The seafloor shows faulting as well. Again, the whole sedimentary column is affected.

Furthermore, we observe an inversion in relief (Figures 5 and 9). While the pre-Oligocene sediments fill basement depressions and are deformed by the basement, a post-early Oligocene drift could develop south of the fault observed between CDPs 8000 and 8100 on line AWI-98004 (Figure 5). These changes in the sedimentary regime can be explained if we consider that the uplifted basement block controlled the path of a palaeo-Antarctic Bottomwater.

Deep crustal structure

A travel-time forward and inverse modelling scheme (Zelt and Smith, 1992) was used to invert picked P-wave travel-time branches for a 2-D velocity-depth model. We included travel-time arrivals with picking uncertainties corresponding to data quality of the respective seismic phases. Phase picking uncertainties lie between 80 and 200 ms (Figure 10a). Initial 2-D modelling started from a trapezoidal grid consisting of seven layers, of which layer 1 is the water column with a velocity of 1.49 km/s and water depths derived from the coincident multi-channel reflection profile AWI-98100. In order to account for the rugged seafloor and basement topography as well as the effect of spatial sampling corresponding to the OBH station intervals and seismic phase coverage, the model was parameterised with variable horizontal spacing of distance-depth-velocity grid nodes between 1 and 10 km for the second and third layer (top sediments and top basement, respectively). The horizontal grid spacing increased to 10–20 km for deeper basement zones. Dominant direct water wave arrivals appear as first arrivals at offsets smaller than 5 km, thus preventing a clear observation of

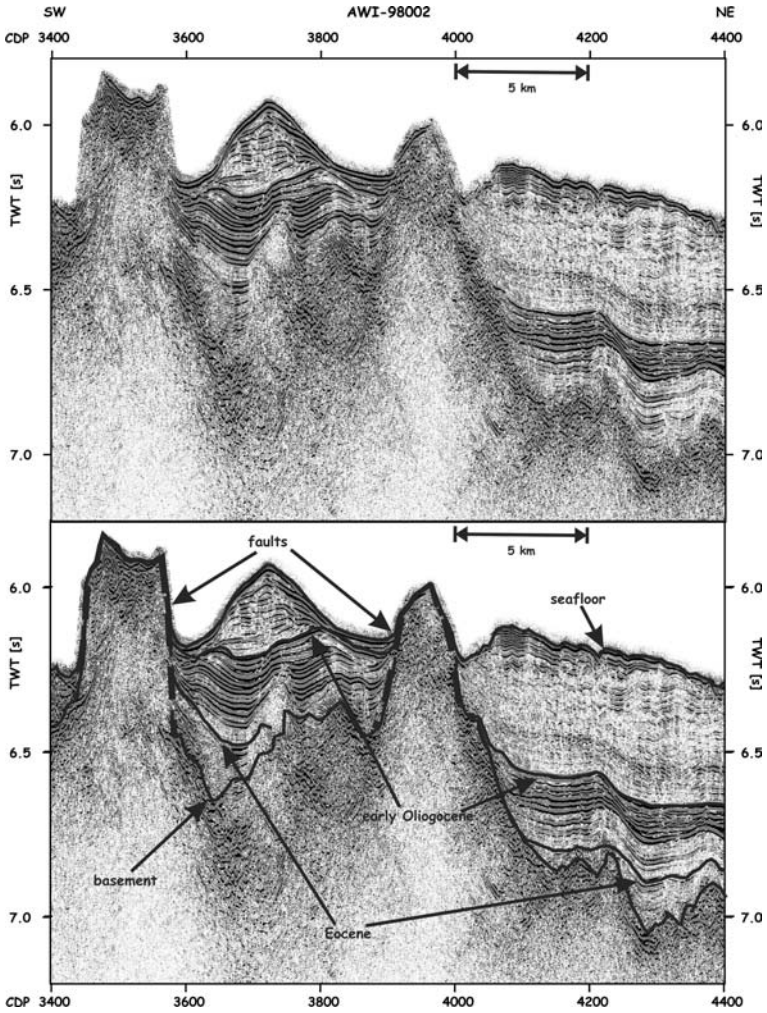

Figure 7. Part of line AWI-98002 showing two basement blocks disrupting sedimentary layers and the seafloor. A drift could develop between the two basement blocks. For location, see Figure 1. Seismostratigraphy was derived via a correlation with ODP Leg 177 Sites 1088, 1089 and 1090 (Wildeboer Schut et al., 2002).

refraction arrivals from the uppermost sedimentary layers or uppermost basement where the station sat on basement. We therefore used the depth and interval velocity information from the sedimentary layer sequence as well as the top of basement observed in the multi-channel reflection profiles for parameterisation of the velocity-depth model.

Forward modelling through ray-tracing in a layer stripping approach from top to bottom was carried out first to reduce the initial large differences between observed and calculated travel-times by adjusting model parameters in a realistic manner (Figure 10b). Reflection and refraction/diving P-wave arrivals from the top basement to mid and lower crust as well as some P_n mantle arrivals constrain the model. Once we achieved a reasonable fit of observed travel-times within or close to the picking error bounds of the observed data, we applied a damped least-square inversion algorithm (Zelt and Smith, 1992) to the travel-time data for grid cells which are covered by rays from at least two different stations as a method of fine-tuning the best fit for those more constrained nodes of the model. However, the lack of reversely covering rays for a number of grid cells leaves parts of the model, mainly toward the ends of the model, only poorly constrained.

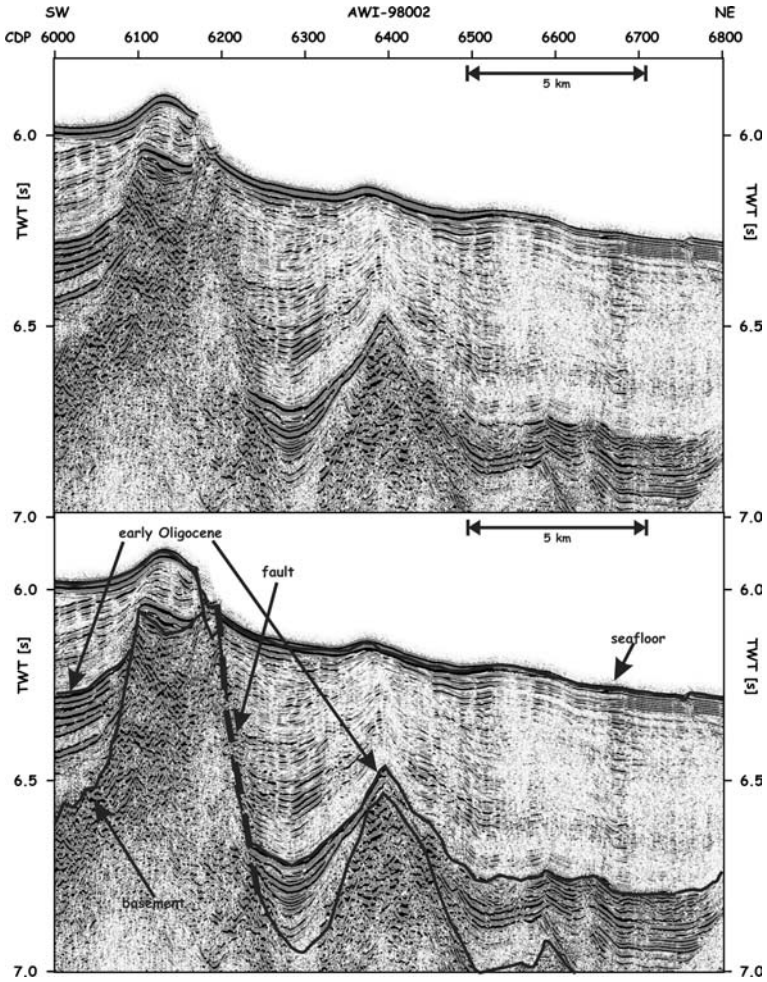

Figure 8. Part of line AWI-98002 showing a basement high disturbing the sedimentary column and another basement high disrupting the layers. For location, see Figure 1. Seismostratigraphy was derived via a correlation with ODP Leg 177 Sites 1088, 1089 and 1090 (Wildeboer Schut et al., 2002).

The final P-wave velocity-depth model along profile AWI-98100 (Figure 10c) includes a thin, and across the ridges almost absent, sedimentary cover with seismic velocities of 1.8–2.0 km/s as observed from the near-vertical reflection data. Basement velocities start with 5.0–5.5 km/s at the top and reach 5.7–6.0 km/s in the upper crust. Mid-crustal velocities range from 6.0 to 6.5 km/s, while lower crustal velocities increase from 6.6 to 6.8 km/s northwest of the northern ridge segment and up to 7.2 km/s in the crust southeast of the ridge valley. While P_mP and P_n arrivals constrain normal oceanic crustal thickness of 6–7 km below seafloor (b.s.f.) for undisturbed crust north and south of the Agulhas Ridge, the ridge itself shows a different deep crustal structure. Moho reflections and lower crustal diving waves, in particular from OBH stations 2 and 4, indicate a deepening of the lower crust below the northern ridge segment resulting in total crustal thickness of 12–13 km (b.s.f.). The average crustal velocity under this ridge segment remains low with 6.1–6.2 km/s, which results from a 5 to 6 km thick upper crust of 5.0–5.8 km/s velocity. Surprisingly, no such overthickened crust is observed underneath the southern ridge segment. There, and under the central ridge valley, the Moho remains flat at about 7–8 km depth b.s.f.

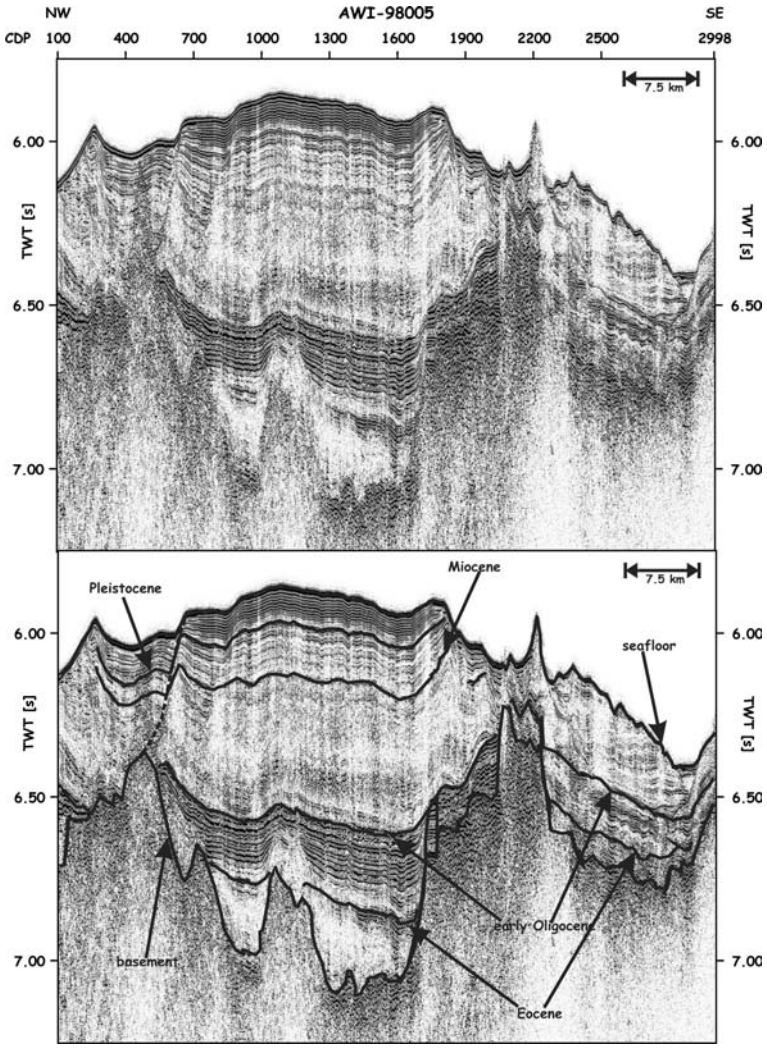

Figure 9. Part of line AWI-98005. A drift developed on top of filled basement topography, thus inversing the relief. For location, see Figure 1. The seismostratigraphy was derived via a correlation with ODP Leg 177 Sites 1088, 1089 and 1090 (Wildeboer Schut et al., 2002).

Discussion

We have seen that, within the Cape Basin, the basement and part of the sedimentary layers in parts are strongly deformed. This points towards the effect of a combined tectono-magmatic activity, which led to the formation of basement ridges parallel to the Agulhas Ridge. As, at least, the pre-Oligocene sedimentary column is affected by deformation, we infer that the renewed activity began in the early Oligocene. The Agulhas Ridge is presently an aseismic structure since no earthquakes have been reported in the Agulhas and Cape Basins region to date (IRIS Data Management Center). In order to understand the structures observed in the seismic lines, several possible causes may be discussed: (a) the influence of a hotspot, (b) ridge jumps, and (c) modifications in spreading rate and direction.

Influence of a hotspot

The Agulhas Falkland Fracture Zone is located close to the inferred Mesozoic tracks of two hotspots. According to hotspot tracks by Martin (1987), the Bouvet Hotspot followed the western

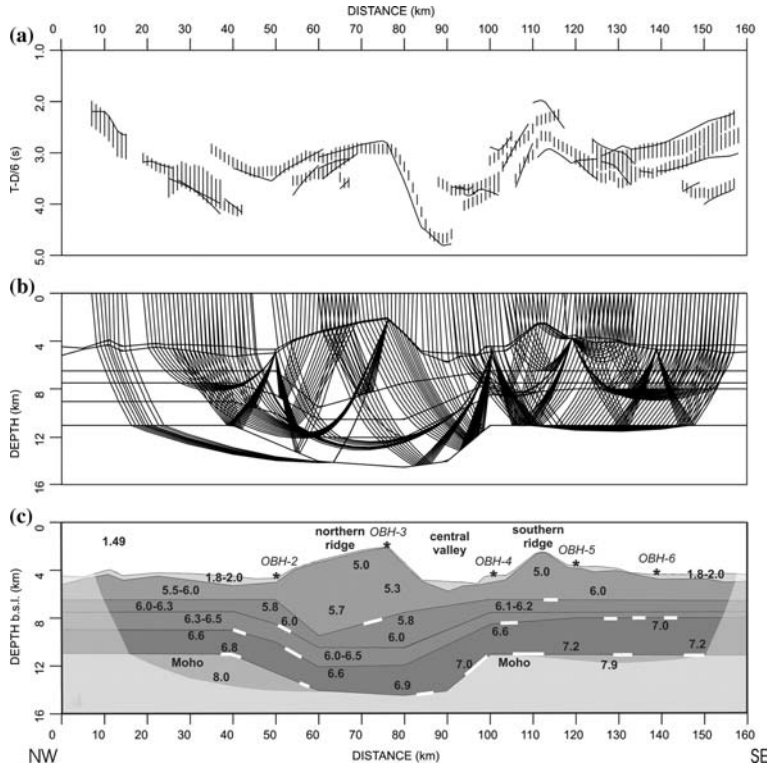

Figure 10. P-wave velocity-depth model along profile AWI-98100. (a) Fit of calculated to observed travel-time branches of all OBH records. The picking uncertainties of observed travel-times are marked with vertical bars. (b) Ray-paths for fitted travel-times. (c) Distribution of seismic velocities (in km/s). Observed reflections from layer boundaries are marked with white lines. The grey-transparent zone indicates unresolved model areas. OBH stations are marked with asterisks.

flank of the Agulhas Plateau from 80 to 69 Ma (Figure 1). Hartnady and le Roex (1985) place the 64 Ma location of the Bouvet Hotspot even farther west near 45°S and 19°E (Figure 1). The track of the Shona Hotspot is inferred to have lain even closer to the Agulhas Ridge (Hartnady and le Roex, 1985; Martin, 1987; Figure 1). The thus available magma could have been channelled towards both the Agulhas Rift and the Agulhas Ridge. Unfortunately, although both hotspots supplied the Agulhas Rift and the Agulhas Ridge with excess material, which in turn may have led to the unusual topography of this part of the Agulhas Falkland Fracture Zone, the activity is too old to account for the observed basement highs and disturbed early Oligocene sediments.

Kempe and Schilling (1974) report that the oldest part of the Discovery Hotspot chain appears to have been formed at about 25 Ma, based on K–Ar ages for the Discovery Tablemount, which is located at ~42°S and 2°E, not far from the Agulhas Ridge (Kempe and Schilling, 1974; Favela and Anderson, submitted paper). This age fits well with a generally observed increased hotspot activity in the African plate (O'Connor et al., 1999). Furthermore, from samples taken near the Mid-Atlantic Ridge (MAR) Douglass et al. (1999) postulate a dispersion of Discovery plume material along the southern edge of the AFFZ from 35 to about 13 Ma. According to their observations the Discovery Hotspot is responsible for the formation of the Eastern Seamounts (about 46°S and 0°E). However, basalts north of the AFFZ exhibit Discovery influence as well. Douglass et al. (1999) interpret this to indicate that while a large amount of the Discovery plume material has been deflected south, some of the material is presently reaching the MAR axis north of the AFFZ. Small (1995) further argues that the relative decrease in lithospheric thickness southward

across the AFFZ would promote migration of buoyant plume material across the fracture zone. Plume material may also be channelised eastward along the fracture zone thereby additionally supplying the Agulhas Ridge with magmatic material. The Discovery Hotspot hence may have been the origin for a renewed volcanic activity north of the Agulhas Ridge in early Oligocene times, especially since the distance Agulhas Ridge – Discovery Seamounts was much smaller at that time.

Ridge jumps

The opening of the South Atlantic was characterised by a number of ridge jumps, which favoured the formation of a large offset (1200 km) along the Agulhas Falkland Fracture Zone. The initial rifting ($\sim$ 133 Ma) was located in the Natal Valley (Tucholke et al., 1981; Ben Avraham et al., 1997). The spreading centre then migrated to 28°E (northern Agulhas Plateau, M0 = $\sim$110 Ma), where an RRR-triple junction was formed under the influence of the Bouvet Hotspot (Tucholke et al., 1981; Martin, 1987; Marks and Stock, 2001). At around 83 Ma another ridge jump placed the spreading axis in the Agulhas Basin west of the Agulhas Plateau (Tucholke et al., 1981; Ben Avraham et al., 1997). Spreading there ceased at Anomaly A 27 (61.2 Ma) when production of seafloor was taken up along the Meteor Rise/Islas Orcadas Rise axis (Tucholke et al., 1981; Marks and Stock, 2001).

As ridge jumps have occurred recurrently, thereby changing the tectonic stress field, they may account for the anomalous bathymetry of the Agulhas Ridge and the rough basement topography. However, the recent most of these ridge jumps is reported to have taken place 61.2 Ma. Thus, this mechanism cannot have been responsible for the post-early Oligocene reactivation we observe.

Changes in spreading rate and direction

The tectonic uplift of crustal blocks may lead to the formation of so called transverse ridges (Keary and Vine, 1996). Transverse ridges are often found in association with major fracture zones and constitute topographic anomalies, that run parallel to the fractures on one or both of their flanks. According to Bonatti (1978) transverse ridges cannot be explained by normal processes of lithosphere accretion. Both compressional and tensional horizontal stresses across the fracture zone, which originate from small changes in the direction of spreading, result in the tectonic uplift of crustal blocks (Bonatti, 1978). This then leads to a transform movement, which is no longer orthogonal to the spreading ridge. Episodic compression and extension arising from several small changes in spreading direction affect different parts of the fracture zone. This has led to the emergence of parts of transverse ridges as islands as reported for St Peter Paul Fracture Zone (Bonatti and Crane, 1984). The Romanche and Vema Fracture Zones constitute two further examples of this process. Vertical motions were initiated by a combination of compressional and tensional forces and resulted in the uplift of upper mantle/crustal blocks near the fracture zones (Bonatti et al., 1977, 1983).

The ridge jumps observed in the South Atlantic at 110, 83, and 62 Ma certainly led to modifications in both spreading direction and rate. Two of those spreading axes were located near the Agulhas Ridge (at the north-eastern and southern end of the ridge) and thus directly affected the ridge. So, following the arguments of Bonatti (1978) we may classify the Agulhas Ridge as a transverse ridge and observe similarities to both Romanche and Vema Fracture Zones (Bonatti et al., 1977, 1983). Furthermore, Marks and Stock (2001) observe an asymmetry in spreading in the Agulhas Basin between anomalies 33o (79.1 Ma) and 34y (83 Ma). They report spreading rates of 2.38 cm/y for the western Agulhas Basin and 4.33 cm/y for the eastern basin without explaining the asymmetry and the adjustment after anomaly 33o. Still, the asymmetry and later adjustment of spreading rates could have added to the anomalous topography of the Agulhas Ridge.

O'Connor et al. (1999) found evidence for a significant deceleration of the African Plate motion relative to a fixed hot spot frame since at least 19 Ma. Considering data from the Tristan/Gough Hotspot chain this could have occurred as early as 30 Ma (early Oligocene). They interpret the increased number of oceanic African hotspots between $\sim$19 and 30 Ma to also point to a link between major changes in plate motion

and the onset and continuation of oceanic hotspot volcanism. The onset of the deceleration of the African Plate and increasing hotspot activity coincides with the oldest deformation of the sedimentary sequence, which we observe in our seismic data. Hence, we interpret the modification in African Plate motion as at least one possible origin of the tectono-magmatic reactivation of the Agulhas Ridge.

Is part of the Agulhas Ridge formed by a sliver of continental lithosphere?

Most studies of the seismic velocity structure of oceanic transform and fracture zones concentrate on the areas to close the active ridge segments where thermal effects of the upwelling asthenosphere are dominant (e.g. Begnaud et al., 1997). Grin'ko et al. (2001) published a velocity model of low resolution from the Murray Fracture Zone of the northern Pacific in which the thickness of the crust increases from 4 to 5 km in the 30 Ma oceanic segment to the south up to 7–8 km for the 46 Ma crust to the north of the fracture zone. Their velocity distribution corresponds to standard ocean crustal velocities with an average of 6.4–6.5 km/s. We observe the same crustal thickness of 6–7 km on either side of the AFFZ, except for the crust beneath the northern ridge which deepens by 3 km and which shows an average crustal velocity lower than that of typical oceanic crust.

Although the processes described in the previous chapters could have led to the formation of increased topography in this segment of the Agulhas Fracture zone, the asymmetric deep crustal structure of the ridge segments and the seismic velocity-depth distribution call for an additional explanation. The ocean crust in the Cape Basin at the northern part of line AWI-98100 lies in the Cretaceous magnetically quiet period, but can be estimated to be about 95–90 Ma old by interpolating between chrons 34y and M0. South Atlantic reconstructions show that by this time, the Maurice Ewing Bank, as part of the greater Falkland Plateau, was moving westward along the Cape Basin in strike-slip motion. The low crustal velocities and the overthickened crust of the northern Agulhas Ridge segment (Figure 10c) can be explained if we assume a "continental" composition. It is possible that a small sliver of continental lithosphere remained attached to the oceanic lithosphere at the northern flank of the actual fracture zone. Even the north-eastern plateau, which extends only north of the central valley (Figure 2a), might be a small continental fragment that split off the Falkland Plateau. However, sampling and analyses of oldest sediments and basement rocks from the Agulhas Ridge segments and its plateau are needed and may provide proof for this speculative idea. Bonatti (1990), Bonatti et al. (1996) and Gasperini et al. (2001) showed that older oceanic and even continental lithosphere may become trapped within younger oceanic lithosphere along transform faults of the equatorial Atlantic in a scenario in which ridge jumping and transform migration provide the mechanism. The series of parallel basement ridges along the AFFZ indicate that the transform fault axis may have migrated within a range of 50–100 km and, therefore, would allow the entrapment of older continental lithosphere.

Conclusions

The interpretation of a set of high-resolution seismic reflection and one seismic refraction/wide angle profiles led to the classification of the Agulhas Ridge as the transverse ridge of the Agulhas-Falkland Fracture Zone (AFFZ). The Agulhas Ridge has undergone tectonic uplift due to episodes of compression and extension, probably caused by small changes in spreading rate and direction and asymmetric spreading of the Mid-Atlantic ridge axis.

We interpret the anomalous topography of the Agulhas Ridge with a large plateau in the northwest and two parallel, up to 2.5 km high segments in the southwest as the result of the influence of three hotspots on the development of the ridge's structure. Both Bouvet and Shona Hotspots passed below the Agulhas Ridge between 80 and 69 Ma (Martin, 1987) or 100 and 64 Ma (Hartnady and le Roex, 1985) and probably caused excess material supplied to this part of the AFFZ.

We further observe an asymmetry in the crustal structure of the ridge segments. The deep crust of the northern ridge is characterised by overthickening and a relative low average crustal

velocity, which we associate with possible continental composition. This may indicate that a small sliver of continental lithosphere was severed off the Maurice Ewing Bank and became attached to this part of the AFFZ in its westward motion during the opening of the South Atlantic Ocean.

The Discovery Hotspot showed first activities around 25 Ma. Discovery plume material migrated southwards across the fracture zone, and we infer that it has been channelised towards the Agulhas Ridge as well, thus tectono-magmatically reactivating the structure. There, the plume material led to the development of basement highs, which disturbed and disrupted the sedimentary layers at least up to early Oligocene.

To shed more light on the initial development and later structural adjustment of the Agulhas Ridge petrological samples are needed to provide ages and, via geochemical analyses, the origin of the magmatic material.

Acknowledgements

We acknowledge with gratitude the cooperation of the captain and crew of the Russian MV Petr Kottsov who made it possible to obtain the seismic data. Many thanks go to E. Wildeboer Schut for meticulously processing the seismic reflection data. Further thanks go to an anonymous reviewer and the guest editor for their careful and helpful comments. The project SETARAP was funded by the German *Bundesministerium für Bildung und Forschung* (BMBF) under contract No. 03G0532A. This research used samples and/or data provided by the Ocean Drilling Program (ODP). The ODP is sponsored by the U.S. National Science Foundation (NSF) and participating countries under management of Joint Oceanographic Institutions (JOI), Inc. This is Alfred-Wegener-Institut publication No. awin14842.

References

Barker, P.F., 1979, The history of the ridge-crest offset at the Falkland-Agulhas Fracture Zone from a small-circle geophysical profile, *Geophy. J. R. astr. Soc.* **59**, 131–145.

Begnaud, M.L., McClain, J.S., Barth, G.A., Orcutt, J.A. and Harding, A.J., 1997, Velocity structure from modeling of the eastern ridge-transform intersection area of the Clipperton Fracture Zone, East Pacific Rise, *J. Geophys. Res.* **102**, (B4), 7803–7820.

Ben Avraham, Z., Hartnady, C.J.H., and Malan, J.A., 1993, Early tectonic extension between the Agulhas Bank and the Falkland Plateau due to the Lafonia microplate, *Earth Planet. Sci. Lett.* **117**, 43–58.

Ben Avraham, Z., Hartnady, C.J.H. and Kitchin, K.A., 1997, Structure and the tectonics of the Agulhas-Falkland fracture zone, *Tectonophysics* **282**, 83–98.

Bird, D., 2001, Shear margins: continent-ocean transform and fracture zone boundaries, *Lead. Edge* 150–159.

Bonatti, E., 1978, Vertical tectonism in oceanic fracture zones, *Earth Planet. Sci. Lett.* **37**, 369–379.

Bonatti, E. 1990, Subcontinental mantle exposed in the Atlantic Ocean on St Peter-Paul islets, *Nature*, **345**, 800–802.

Bonatti, E. and Crane, K., 1984, Oceanic fracture zones, *Sci. Am.* **250**, 36–47.

Bonatti, E., Ligi, M., Borsetti, A.M., Gasperini, L., Negri, A. and Sartori, R., 1996, Lower Cretaceous deposits trapped near the equatorial Mid-Atlantic Ridge, *Nature* **380**, 518–520.

Bonatti, E., Sarnthein, M., Boersma, A., Gorini, M. and Honorez, J, 1977, Neogene crustal emersion and subsidence at the Romanche Fracture Zone, equatorial Atlantic, *Earth Planet. Sci. Lett.* **35**, 369–383.

Bonatti, E., Sartori, R. and Boersma, A., 1983, Vertical crustal movements at the Vema Fracture Zone in the Atlantic: evidence from dredged limestones, *Tectonophysics* **91**, 213–232.

Cande, S.C., LaBrecque, J.L., Larson, R.L., Pitman, III, W.C., Golovchenko, X. and Haxby, W.F., 1989, *Magnetic lineations of the worlds ocean basins (map),* Am. Ass. Petr. Geol., Tulsa, USA.

Detrick, R.S., White, R.S. and Purdy, G.M., 1993, Crustal structure of the North Atlantic fracture zones, *Rev. Geophy.* **31**, 439–458.

Douglass, J., Schilling, J.-G. and Foutignie, D., 1999, Plume-ridge interactions of the Discovery and Shona mantle plumes with the southern Mid-Atlantic Ridge (40°–55°S), *J. Geophys. Res.* **104** (B2), 2941–2962.

Favela, J. and Anderson, D.L., Extensional tectonics and global volcanism, *Conference Proceedings*, Erice, Italy. in review.

Gasperini, L., Bernoulli, D., Bonatti, E., Borsetti, A.M., Ligi, M., Negri, A., Sartori, R. and von Salis, K., 2001, Lower Cretaceous to Eocene sedimentary transverse ridge at the Romanche Fracture Zone and the opening of the equatorial Atlantic, *Mar. Geol.*, **176**, 101–119.

Gersonde, R., Hodell, D.A. and Blum, P. et al. (eds.), 1999, *Proceedings of the Ocean Drilling Program, Initial Reports* 117 [CD-ROM]. Available from: Ocean Drilling Program, Texas A&M University, College Station, TX 77845–9547, USA.

Grin'ko, B.N., Neprochov, Y.P. and Protkov, V.V., 2001, Wave fields and crustal structure of the northeastern basin of the Pacific Ocean in the Murray Fracture Zone region from the data of seismic studies, *Oceanology* **41**, 580–588.

Hartnady, C.J.H. and le Roex, A.P., 1985, Southern Ocean hotspot tracks and the Cenozoic absolute motion of the African, Antarctic, and South American plates, *Earth Planet. Sci. Lett.* **75**, 245–257.

IRIS Data Management Center, http://www.iris.washington.edu.SeismiQuery/events.html.

Kastens, K., 1987, A compendium of causes and effects of processes at transform faults and fracture zones, *Rev. Geophys.* **25**, 1554–1562.

Keary, P. and Vine, F.J., 1996, *Global tectonics*, Blackwell Science Ltd, Oxford, 333 p.

Kempe, D. and Schilling, J.-G., 1974, Discovery Tablemount basalt: petrology and geochemistry, *Contrib. Mineral. Petrol.* **44**, 101–115.

Labreque, J.L. and Hayes, D.E., 1979, Seafloor spreading history of the Agulhas Basin, *Earth Planet. Sci. Lett.* **45**, 411–428.

Lorenzo, J.M. and Wessel, P., 1997, Flexure across a continent-ocean fracture zone: the northern Falkland/Malvinas Plateau, South Atlantic, *Geo-Mar. Lett.* **17**, 110–118.

Marks, K.M. and Stock, J.M., 2001, Evolution of the Malvinas Plate south of Africa, *Mar. Geophys. Res.* **22**, 289–302.

Martin, A.K. 1987, Plate reorganisations around Southern Africa, hot-spots and extinctions, *Tectonophysics* **142**, 309–316.

Martin, A.K. and Hartnady, C.J.H., 1986, Plate tectonic development of the southwest Indian Ocean: a revised reconstruction of east Antarctica and Africa, *J. Geophys. Res.* **91**, 4767–4786.

O'Connor, J.M., Stoffers, P., van den Bogaard, P. and McWilliams, M., 1999, First seamount age evidence for significantly slower African Plate motion since 19–30 Ma. *Earth Planet. Sci. Lett.* **171**, 575–589.

Small, C., 1995, Observations of ridge-hotspot interaction in the Southern Ocean. *J. Geophys. Res.* **100** (B9), 17931–17946.

Smith, W.H.F. and Sandwell, D.T., 1997, Global seafloor topography from satellite altimetry and ship depth sounding, *Science* **277**, 1956–1962.

Tucholke, B.E., Houtz, R.E. and Barrett, D.M., 1981, Continental crust beneath the Agulhas Plateau, southwest Indian Ocean, *J. Geophys. Res.* **86**, 3791–3806.

Wildeboer Schut, E., Uenzelmann-Neben, G. and Gersonde, R., 2002, Seismic evidence for bottom current activity around the Agulhas Ridge, *Global Planet. Change* **34**, 185–198.

Zelt, C.A. and Smith, R.B., 1992, Seismic traveltime inversion for 2-D crustal velocity structure, *Geophys. J. Int.* **108**, 16–34.